The Influence of $^{14}N(e^-,\nu)^{14}C(\alpha,\gamma)^{18}O$ reaction on the He-Ignition in Degenerate Physical Conditions

Luciano Piersanti [1]
Dipartimento di Fisica dell'Università degli Studi di Napoli "Federico II", Mostra d'Oltremare, pad. 20, 80125, Napoli, Italy; lpiersanti@astrte.te.astro.it

Santi Cassisi
Osservatorio Astronomico di Teramo, Via M.Maggini 47, 64100 Teramo, Italy; cassisi@astrte.te.astro.it

and

Amedeo Tornambé [2]
Osservatorio Astronomico di Teramo, Via M.Maggini 47, 64100 Teramo, Italy; tornambe@astrte.te.astro.it

[1]Osservatorio Astronomico di Teramo, Via M.Maggini 47, 64100 Teramo, Italy
[2]Dipartimento di Fisica, Università de L'Aquila, Via Vetoio, 67100 L'Aquila, Italy

ABSTRACT

The importance of $^{14}N(e^-,\gamma)^{14}C(\alpha,\gamma)^{18}O$ (NCO) chain on the onset of the He-flash in degenerate physical conditions has been reevaluated. We find that low-mass, metal-rich (Z $\geq$ 0.001) structures climbing the Red Giant Branch do never attain the physical conditions suitable for the onset of this chain, while at lower metallicities the energy contribution provided by NCO reaction is too low to affect the onset of the central He-flash.

At the same time, our evolutionary models suggest that for a Carbon-Oxygen White Dwarf of mass $M_{WD} = 0.6M_\odot$ accreting He-rich matter, directly or as a by-product of an overlying H-burning shell, at rates suitable for a dynamical He-flash, the NCO energy contribution is not able to keep hot enough the He-shell and in turn to avoid the occurrence of a strong electron degeneracy and the ensuing final explosion.

Subject headings: nucleosynthesis - stars: accretion - supernovae: general - white dwarf

1. Introduction

More than 25 years ago Mitalas (1974) firstly suggested that the $^{14}N(e^-,\gamma)^{14}C(\alpha,\gamma)^{18}O$ (NCO) reaction could play an important role on the onset of the He-flash in the He core of a Red Giant (RG) star. In fact in high degenerate physical conditions, when the electron Fermi energy becomes of the order of the energy threshold for electron capture on ^{14}N ($\sim$ 156 keV), a significant amount of ^{14}C can be produced. It is important to notice that ^{14}C is unstable for β^- decay, so that only for densities greater than a critical value ($\rho_{th} = \rho Y_e \sim 10^6$ g/cm^3, where ρ is the mass density and Y_e is the number of electrons per baryon) ^{14}C lives long enough to undergo an α-capture. The latter reaction heats up the inner zones of the He core in such a way that the physical conditions suitable for the ignition of He-burning are attained before when compared with structures in which the NCO energy contribution is neglected. This implies that the He core mass at the onset of the central He-flash could be reduced and, as a consequence, the luminosity of both tip of RGB and Horizontal Branch (HB) could be fainter. This notwithstanding the main conclusion reached by Mitalas is that NCO reaction does not affect at all the evolution of a RG Population II star because the typical physical conditions of the He core do not allow the onset of electron capture.

However, Kaminisi, Arai & Yoshinaga (1975) pointed out that Mitalas underestimated the cross section of the α-capture on ^{14}C by a factor 10^6. Moreover, Kaminisi & Arai (1975) compared the energy released by the $^{14}N(e^-,\gamma)^{14}C(\alpha,\gamma)^{18}O$ chain and by 3α reaction respectively and concluded that NCO chain dominates over the 3α reaction for central temperatures and densities typical of a low metallicity RG star.

A new evaluation of the role played by NCO chain has been made by Spulak (1980). He pointed out that the onset of this reaction critically depends on the density so that its energy contribution is strongly concentrated toward the center of the He core in a RG structure, while the core He-flash driven by 3α occurs at the mass point where the temperature is maximum, which is off-center and approximately located at $M_{T-max} \sim 0.15 M_\odot$. By accounting for the energy balance between the NCO chain, neutrino losses and 3α reaction, Spulak concluded that NCO chain is not able to trigger the onset of the He-flash because in a typical low metallicity RG star the central density becomes high enough to trigger the electron capture when the 3α reaction has already ignited off center and its energy contribution is quite relevant.

In 1984 Hashimoto, Nomoto, Arai & Kaminisi (Hashimoto et al. 1984) recomputed the cross section for the electron capture on ^{14}N and once again they concluded that NCO reaction dominates over 3α reaction in the ignition of the He-flash. They also pointed out that the key role played by this reaction strongly depends on the chemical composition of

the He core when the central density exceeds the density threshold for the electron capture. Using this updated cross section, Hashimoto et al. (1986) showed that NCO reaction plays an important role in the onset of the He-flash in He WDs accreting Helium rich matter directly or as a by-product of an overlying H-burning shell. Moreover, these authors pointed out that NCO reaction also affects the evolution of a CO WD accreting He rich matter directly or as a by-product of H-burning. In fact, for low accretion rates (i.e. smaller than $4 \times 10^{-8}\ M_\odot\ \mathrm{yr}^{-1}$) the energy contribution provided by NCO reaction heats up the He layers, thus preventing them to undergo a violent dynamical He-flash and causing an increase in the mass of the CO core up to the Chandrasekhar mass limit.

For this reason, Woosley & Weaver (1994) included NCO chain in their nuclear network to construct the pre-supernova model of cool CO WDs accreting He rich matter. Their calculations show that NCO reaction does not affect the final outcome of the process (He detonation), since the main effect is a slight decrease in the mass of the He layer at the onset of the flash.

More recently Piersanti et al. (1999) have included the NCO chain in the computation of the evolution of a low mass CO WD accreting He rich matter both directly and as a by-product of H-burning shell at rates suitable for the occurrence of a He detonation. They found that the differences produced by NCO chain are quite negligible and pointed out that this result is due to the fact that their initial WD model is an evolutionary one, obtained evolving an intermediate mass star with a moderate mass loss from the Zero Age Main Sequence down to the cooling sequence. In such a model there is no ^{14}N available for NCO reaction at the physical base of the He-shell where the He-flash is ignited.

In order to improve our knowledge on the role played by NCO chain in the framework of stellar evolution we have included this chain in our nuclear network, and performed several numerical experiments on low mass stars climbing the RGB, on central He-burning models, as well as on low mass CO WDs accreting He-rich matter. Moreover, we have also analyzed extensively the dependence of the NCO energy contribution on stellar metallicity.

The plane of this paper is the following: in §2 we discuss the numerical techniques, the physical assumptions together with the input physics; in §3 we present the results concerning the evolution along the RGB, while in §4 we discuss the physical and chemical properties of CO WDs and explore the thermal behavior of a CO WD accreting He-rich matter. In §5 a brief discussion and the conclusions close the paper.

2. Physical Inputs

All the models have been calculated with an update version of the FRANEC code (Chieffi & Straniero 1989), the main differences have been discussed in Cassisi et al. (1998). As far as the equation of state (EOS) is concerned, we adopted the EOS computed by Straniero (1988). For low-temperature (T <12000 K) opacities we adopted the tables provided by Alexander & Ferguson (1994) while for higher temperatures the tables provided by Huebner et al. (1977) has been used. During the He burning phase we adopted a nuclear network which includes CO chain ($^{12}C(\alpha,\gamma)^{16}O(\alpha,\gamma)^{20}Ne$), NO chain ($^{14}N(\alpha,\gamma)^{18}O(\alpha,\gamma)^{22}Ne$) and NCO chain ($^{14}N(e^-,\nu)^{14}C(\alpha,\gamma)^{18}O(\alpha,\gamma)^{22}Ne$). All the cross sections are from Caughlan & Fowler (1988) with the exception of $^{12}C(\alpha,\gamma)^{16}O$ for which we adopted the cross section provided by Caughlan et al. (1985, for a detailed discussion on the current uncertainty on this reaction see Bono et al. 2000). The electron capture on ^{14}N was implemented according to Hashimoto et al. (1986). The evolution during the central He burning phase has been computed by taking into account semiconvection but by neglecting breathing pulses (Caputo et al. 1989). The accretion process has been computed by assuming that the accreted matter has the same specific entropy of the matter at the surface of the WD (Limongi & Tornambé 1991). For the heavy elements we assumed a solar scaled distribution (Grevesse 1991).

3. The evolution along the RGB

We have computed three different sets of models at different metallicities, - Z=0.02, 0.001, 0.0001 - from the pre-Main Sequence phase up to the ignition of the central He-burning. For each set of models we adopted three different evolving masses, namely M=0.6, 0.7 and 0.8 $M_\odot$. Fig. 1 shows the $\rho - T$ plane for selected structures at various luminosity levels along the RGB up to the onset of the He-flash (the top curve in each panel). The dashed lines display the evolution of the central conditions of the models, while the heavy solid lines on the right of the tracks mark the region in which e-captures occur. Data plotted in this figure show that at higher metallicities (Z=0.02 and 0.001) the evolving stars do never attain densities high enough for the occurrence of e-captures. In these structures the NCO reaction does not become active at all, and thus it does not provide any contribution to the He-burning. On the contrary, in metal-poor structures (Z=0.0001) the density of the central regions becomes higher than the critical density for the onset of the NCO chain. Therefore its energy contribution might play a role in the He-burning ignition.

To assess in more detail the effect of the NCO reaction in metal-poor structures, Fig. 2 shows the evolution in the $\rho - T$ plane of the central conditions for the 0.6 $M_\odot$ models which

include (dotted line) or neglect (solid line) the NCO chain in the nuclear network. As soon as the central density exceeds the critical value ρ_{th} ($\log(L/L_\odot) = 3.259$, $\log(T_e) = 3.643$), the electron capture becomes active and produces ^{14}C; the subsequent α-capture on ^{14}C releases some amount of energy that heats up the center. However the abundance of ^{14}N nuclei is very low ($X_{^{14}N} < 10^{-4}$ by mass) and, in addition, the energy lost via neutrino emission are always active, and therefore the center is barely heated. The top left panel of Fig. 1 clearly shows that, only the innermost zone of the He-core has a density larger than the critical value, and therefore the point where the He-burning is ignited via 3α reaction remains completely unaffected. This implies that at the onset of the He-flash - defined according to Sweigart & Gross (1978) as the time when the energy production in the inner regions is greater than the neutrino energy losses - the He-core mass, and in turn the luminosity of the star are the same compared to the case in which NCO chain is not accounted for (see Fig. 3).

4. CO WDs Accreting Mass

4.1. The Chemical and Physical Properties of CO WDs

To investigate the physical and chemical properties of CO WDs we computed a set of models from the central He burning phase down to the cooling sequence for different metallicities. Figures 4-5 show temperature and density profiles (right panels) together with the chemical abundances in the most external layers (left panels) for each model. Data plotted in the left panels show that the abundance of ^{14}N is equal to zero at the physical base of the He-shell, defined as the zone where the He abundance is Y=0.5 by mass. This is due to the fact that during the previous evolution (He-shell-burning phase) ^{14}N has been transformed into ^{22}Ne via NO chain. In fact, the $^{14}N(\alpha,\gamma)^{18}O$ reaction becomes active at a temperature of the order of 8×10^7 K with a mild dependence on density. As a consequence, the innermost zone of the He-shell is enriched in ^{22}Ne and deprived in ^{14}N .

4.2. Accretion Experiments

As already mentioned (see §1), Woosley & Weaver (1994) included NCO reaction in their nuclear network to compute the evolution of a low-mass CO WD accreting He-rich matter. By comparing their results with those of Limongi & Tornambé (1991), it is evident that for accretion rates suitable for the occurrence of a hydrodynamical event ($\dot{M} < 4 \times 10^{-8}$ $M_\odot$ yr^{-1}), the energy contribution provided by NCO chain marginally affects the evolution

of the accreting models. In fact, the final outcome remains an explosion and the only change is a slight reduction in the mass extension of the He layer at the onset of the He-flash. This result is confirmed by Piersanti et al. (1999) who pointed out that if the initial model of the CO WD is an evolutionary one, then the influence of the NCO chain is negligible due to the lack of ^{14}N at the bottom of the He-shell. The same occurrence takes place over the thick He-layer, surrounding the CO core, where the Helium abundance has not been modified by 3α reaction, but the NO reaction has been active. In addition, these authors noticed that, for a fixed chemical composition of the accreted matter, the energy contribution of NCO chain depends on the accretion rate, however the final outcome remaining unchanged. In fact, a decrease in the accretion rate causes an increase in the He-layer mass at the onset of the He-flash, and an increase in the ignition density as well. Therefore, the ^{14}C shell, defined as the point where the NCO reaction energy release is at maximum, can move outward (in mass) detaching more and more from the base of the He-shell so that the heating induced by the energy delivered by this chain does not affects the point where the He-flash is ignited.

To investigate more in detail this point we have computed an additional set of models in which He-rich matter (Y=0.98 and Z=0.02) is accreted onto a cooled down CO WD at rates suitable for an He detonation ($\dot{M} = 1 \div 4 \times 10^{-8} M_\odot$). The initial model for the CO WD has been obtained by evolving a 0.6 $M_\odot$ pure He star (Y=0.98, Z=0.02) from the He Main Sequence down to the cooling sequence. The luminosity, the effective temperature, the central temperature, and density of this structure are the following: $\log(L/L_\odot) = -1.905$, $\log(T_e) = 4.236$, $\log(T_c) = 7.310$ and $\log(\rho_c) = 6.585$. A glance at the data plotted in Fig. 6 shows that at the physical base of the He-layers the ^{14}N abundance is zero. The main physical parameters at the onset of the He-flash are listed for each model in Table 1: the first column gives the accretion rate ($M_\odot$ yr^{-1}) while the others give the thickness in mass of the He-layers (solar units), the temperature (K), the density (g/cm^3), and the degeneration parameter at the point where the energy production via He-burning attains the maximum value. The quantities referred to the case which neglects the NCO energy contribution are listed in columns 2 to 5, while those referred to the case which includes the NCO reactions are listed in columns 6 to 10.

Fig. 7 shows the evolution in the $\rho - T$ plane of the bottom of the He layer for models computed at different $\dot{M}$ and neglecting the NCO energy contribution. Note that only for accretion rates smaller than 3×10^{-8} $M_\odot$ yr^{-1} the NCO chain could become active. In fact, only for these values of $\dot{M}$ the density at the physical base of the He-shell exceeds ρ_{th} (dashed line).

Fig. 8 depicts the evolution in the $\rho - T$ plane of the base of the He-shell with (dashed

line) and without (solid line) the inclusion of NCO reaction in the nuclear network. The evolution of the mass point where the energy production is at maximum is plotted in Fig. 9. As soon as the density becomes greater than ρ_{th}, the NCO reaction is ignited and releases a small amount of energy. The continuous accretion process causes an increase in the shell density; therefore during the subsequent evolutions the physical conditions suitable for the NCO reaction are reached in more and more external layers. As a matter of fact, a ^{14}C burning shell forms and moves outward in mass all over the accretion process up to the onset of the He-flash.

Interestingly enough, an increase in the accretion rate causes a rapid outward shift of the ^{14}C shell. This occurrence is simply explained by noting that the He-shell is globally less degenerate due to the increase in the accretion rate. Data plotted in Fig. 9, and the physical parameters listed in Table 1, clearly support the evidence that the effects of NCO chain are more relevant at intermediate accretion rates ($\dot{M} = 1.5 \div 2 \times 10^{-8}\ M_{\odot}\ \mathrm{yr}^{-1}$). In fact, at lower accretion rates the He-shell is more degenerate and the ^{14}C shell detaches more and more from the bottom of the He-shell. On the contrary, for higher accretion rates the physical conditions suitable for the electron capture are attained when 3α reaction already produces a huge amount of energy. Even at higher accretion rates (higher than $3 \times 10^{-8}\ M_{\odot}\ \mathrm{yr}^{-1}$) the density of the He-shell does never exceed the critical density ρ_{th}, and therefore the NCO reaction does not supply any energy contribution.

This notwithstanding the inclusion of NCO energy contribution does not change the final fate of these structures, all of them should undergo an explosive event.

5. Final remarks

We have shown that the effect of NCO reaction on the onset of He-burning in degenerate physical conditions is negligible. In fact, for low-mass structures climbing the RGB, the models with high metallicity (Z=0.001 and Z=0.02) do not attain densities so high to ignite the NCO reaction,while more metal-poor models present such a low abundance of ^{14}N that the energy released by α-captures on ^{14}C does not affect the evolution. Of course if the ρ_{th} value was smaller than we assumed then the energy contribution of the NCO chain should be reevaluated. Accounting for this evidence, we have decided to perform several numerical experiments for a $0.8 M_{\odot}$ solar metallicity model, arbitrarily decreasing the value of ρ_{th} in order to test to what extend present results are affected by the uncertainty on this parameter, as well as to verify if stellar observables allow us to put a firm constraint on this quantity. From the data listed in Table 2, it is possible to notice that a decrease of the order of 20% of ρ_{th} has no effect on the evolutionary properties of the model. However, when the

value of ρ_{th} is decreased by a larger factor, the numerical experiments clearly reveal that the size of the He core at the He flash onset and, in turn, the luminosity of the RGB tip and of the ZAHB are significantly affected by the NCO energy release. In particular, for a decrease of 30% of ρ_{th}, we obtain an RGB tip luminosity of $\log(L_{tip}/L_{\odot}) = 3.362$ and an He core mass of $M_{He} = 0.4612\ M_{\odot}$ to be compared with the values of the standard case, namely $\log(L_{tip}/L_{\odot}) = 3.430$ and $M_{He} = 0.4753\ M_{\odot}$. From an observational point of view, we can estimate that this occurrence produces an increase in the visual magnitude of the RGB Tip and of the ZAHB equal to ≈ 0.2 mag and ≈ 0.1 mag, respectively. These values are well within the current observational and theoretical uncertainties which still affect these crucial observables (Cassisi et al. 1998, Salaris & Cassisi 1998). However, a further decrease ($\approx 40\%$) in the value of ρ_{th} (see data in Table 2) produces quite larger effects. These changes could be easily tested, allowing to put a firm constraint on ρ_{th} value, once the sample of high-metallicity clusters with reliable RGB Tip luminosity estimates will be increased.

Following the suggestion of an anonymous referee we also explored the dependence of our results on the value of the $^{14}C(\alpha,\gamma)^{18}O$ cross section. The current scenario (Funck & Langanke 1989; Goerres et al. 1992) states that at low temperatures ($T < 10^8$ K) the cross section for this reaction rate is dominated by a direct capture contribution which is affected by an uncertainty of roughly two orders of magnitude. Owing to this indisputable fact, we performed several numerical experiments by arbitrarily changing the value of the cross section for the α capture on the ^{14}C. In particular, the value of $N_A < \sigma v >_{^{14}C,\alpha}$ by Caughlan & Fowler (1988) has been multiplied by factors equal to 10^{-2}, 10^{-1}, 10^1 and 10^2.

As far as the $M = 0.6 M_{\odot}$ model at $Z = 10^{-4}$ is concerned (see §3), Fig. 10 shows the evolutions of the center in the $\rho - T$ plane. Data plotted in this figure suggest that an increase in the reaction rate of $^{14}C(\alpha,\gamma)^{18}O$ does not cause a significant change in the canonical scenario, except for a slightly faster release of the energy. In particular, it is worth noticing that the profiles associated with an increase of one and two order of magnitude overlap, respectively. This occurrence is a direct consequence of the fact that the efficiency of the NCO cycle is only triggered by the e-capture on ^{14}N. On the other hand, a decrease in the reaction rate of the α capture on the ^{14}C, causes a decrease in the energy released, and in turn an increase in its duration up to the onset of the He-flash. In any case the He-core mass and the luminosity level of the Tip remain unchanged when compared with the standard case.

The same experiments were also performed for the model at $M = 0.8 M_{\odot}$ and $Z = 0.02$ by assuming a decrease of the order of 30% in the transition density for the e-capture. Tab. 3 lists the values of the He core mass, central temperature, and density at the onset of the

He-flash. Once again the increase in the reaction rate of the α capture on the ^{14}C does not cause a significant change of the physical conditions at the onset of the He-flash. On the contrary, a decrease in the value of $N_A < \sigma v >_{^{14}C,\alpha}$ causes a decrease in the degeneration of the He core, and therefore a mild decrease in the He core mass at the onset of the He flash. Unfortunately, the variations in the observables (luminosity level of tip and Horizontal Branch) are too small to constrain the efficiency of this reaction.

In the case of typical mass CO WDs accreting He-rich matter we showed that the final outcome depends only on the accretion rate, while the NCO reaction only causes a slight decrease in the He layers mass at the He-flash. This occurrence implies that the inclusion of the NCO reaction cannot switch an explosive He-burning into a quiescent one in such a way that the CO core can grow in mass up to the Chandrasekhar mass limit. In fact, for low $\dot{M}$ values the energy contribution given by the NCO reaction is not able to heat up the bottom of the He-shell, while for higher accretion rates the physical conditions for the e-capture are never reached.

These considerations are still valid when He-rich matter is accreted as a by-product of a H-burning shell. In fact, for higher accretion rates (higher than 4×10^{-8} $M_\odot$ yr^{-1}) the presence of the H-burning shell increases the temperature of underlying He-shell, thus preventing it to become degenerate. Therefore the physical conditions for the ignition of NCO chain are never attained (Cassisi, Iben & Tornambé 1998). On the contrary, for lower accretion rates He and H shells decouple and the behavior of the models accreting H-rich matter are identical to the models accreting He directly (Piersanti et al.2000).

We wish to warmly thank G. Bono for several suggestions and useful discussion on this topic, as well as for the generous and painstaking effort provided for improving the readability of this paper. Useful comments and suggestions from an anonymous referee are also acknowledged. This work was supported by MURST (Cofin2000) under the scientific project "Stellar observables of cosmological relevance".

REFERENCES

Alexander, D. R. & Ferguson, J. W., 1994, ApJ, 437, 879

Bono, G., Caputo, F., Cassisi, S., Marconi, M., Piersanti, L. & Tornambè, A., 2000, ApJ, 543, 955

Caputo, F., Castellani, V., Chieffi, A. & Tornambé A., 1989, ApJ, 340, 241

Cassisi, S., Castellani, V., Degli Innocenti S. & Weiss, A., 1998 A&ASS, 129, 267

Cassisi, S., Iben, I. Jr. & Tornambè, A., 1998, ApJ, 496, 376

Caughlan, G.R., Fowler, W.A., Harris, M.J. & Zimmerman, B.A., 1985, Atomic Data and Nuclear Data Tables, 32, 197

Caughlan, G.R. & Fowler, W.A., 1988, Atomic Data and Nuclear Data Tables, 40, 283

Chieffi, A. & Straniero, O., 1989, ApJS, 71, 47

Funck, C. & Langanke K., 1989, ApJ, 344, 46

Goerres, J., Graff, S., Wiescher, M., Azuma, R.E., Barnes, C.A. & Wang, T.A., 1992, NP A, 548, 414

Grevesse, N., 1991, Evolution of Stars: The Photospheric Abundance Connection, in Proc. IAU Symp. 145, Michaud, G. & Tutukov A. Eds., Kluwer Academic Publishers, Dordrecht, p.63

Hashimoto, M.A., Nomoto, K.I., Arai, K. & Kaminisi, K., 1984, Phys. Rep. Kumamoto Univ., 6, 75

Huebner, W.F., Merts, A.L., Magee, Jr. M.H.. & Argo, M.F., 1977, Los Alamos, Sci. Lab. Rep. LA-6760-M

——, 1986, ApJ, 307, 687

Kaminisi, K. & Arai, K., Phys. Rep. Kumamoto Univ., 1975, 2, 19

Kaminisi, K., Arai, K. & Yoshinaga, K., 1975, Phys. Rep. Kumamoto Univ., 53, 1855

Limongi, M. & Tornambé, A., 1991, ApJ, 371, 317

Mitalas, R., 1974, ApJ, 187, 155

Piersanti, L., Cassisi, S., Iben, I.Jr. & Tornambé, A., 1999, ApJ Lett., 521, L59

——, 2000, ApJ, 535, 932

Salaris, M. & Cassisi, S., 1998, MNRAS, 298, 166

Sweigert, A.V. & Gross, P.G., 1978, ApJSS,36 405

Spulak, R.G. Jr., 1980, ApJ, 235, 565

Woosley, S.E. & Weaver, T.A., 1994, ApJ, 423, 371

This preprint was prepared with the AAS LaTeX macros v4.0.

Fig. 1.— Profiles in the $\rho-T$ plane of stars climbing the RGB up to the onset of the central He-flash. For each evolving mass of fixed metallicity (see labeled values) physical properties at different luminosity levels are plotted. The model at the He ignition is the top line. The dashed line shows the evolution as a function of time of the physical conditions at the center. The heavy solid line on the right of each panel marks the region suitable for electron capture to occur: for structures located at the right of this line e-captures occurs.

Fig. 2.— The evolution in the $\rho - T$ plane of the center of the model with M=0.6 $M_{\odot}$ and Z=0.0001. The solid lines refer to the model in which the NCO energy contribution is not taken into account, while the dashed one refers to the model which includes of the energy contribution given by NCO reaction.

Fig. 3.— Time evolution of the He-core mass for the model at M=0.6 $M_{\odot}$ and Z=0.0001. Dashed and solid lines refer to models in which the NCO energy contribution has been included and neglected respectively.

Fig. 4.— Chemical abundances in the most external layers of the He-shell (left panels) and profiles in the $\rho-T$ plane (right panels) for models of CO WDs obtained evolving structures with Z=0.02, Y=0.298, mass of the He-core of 0.475 $M_{\odot}$, and different total masses (see labeled values) from the Zero Age Horizontal Branch down to the cooling sequence. The values of luminosity, effective temperature, central temperature, and density for each model are plotted in the right panels. In the left panels the solid line refers to $\log(^{4}He)$, the dotted one to $\log(^{12}C)$, the short-dashed one to $\log(^{14}N)$, and the long-dashed one to $\log(^{16}O)$.

Fig. 5.— The same as in Fig. 4, but for the case Z=0.001 and Y=0.244.

Fig. 6.— Chemical abundances in the most external layers of a 0.6 $M_{\odot}$ CO WD (see text for more details).

Fig. 7.— The evolution in the $\rho - T$ plane of the physical base of the He-shell for models accreting He-rich matter with solar metallicity at different accretion rates (as labelled) onto a cooled down CO WD of 0.6 $M_{\odot}$.

Fig. 8.— The evolution in the $\rho - T$ plane of the physical base of the He-shell for models accreting He-rich matter at different accretion rates (as labelled). The solid lines refer to the case in which the NCO energy contribution is not take into account, while the dashed ones to the case in which NCO reaction has been included in the nuclear network.

Fig. 9.— The evolution of the mass point where the energy production is maximum as function of time. The dashed and solid lines show models in which NCO energy contribution is included and neglected respectively.

Fig. 10.— Evolution in the $\rho - T$ plane of the center of the model with M=0.6 $M_{\odot}$ and Z=0.0001 in which the energy contribution given by NCO reaction has been taken into account. Individual lines refer to different values adopted for the $^{14}C(\alpha, \gamma)^{18}O$ cross section as labelled inside the figure (see text).

Table 1. Accretion of He-rich matter onto a CO WD of M=0.6 $M_{\odot}$.

$\dot{M}$	ΔM_{He}	$\log(T_{He})$	$\log(\rho_{He})$	ψ	ΔM_{He}	$\log(T_{He})$	$\log(\rho_{He})$	ψ
	without NCO				with NCO			
10^{-8}	0.443	7.877	6.932	75	0.436	7.883	6.905	71
1.5×10^{-8}	0.393	7.895	6.742	57	0.363	7.903	6.648	50
2×10^{-8}	0.271	7.933	6.230	27	0.244	7.932	6.163	25
2.5×10^{-8}	0.204	7.950	5.965	18	0.203	7.953	6.008	19
3×10^{-8}	0.174	7.966	5.805	14	-	-	-	-
4×10^{-8}	0.142	7.994	5.623	10	-	-	-	-

Table 2. The effect of different reduction factor of ρ_{th} on the evolution of a 0.8 $M_{\odot}$ Z=0.02 model.

$\frac{\Delta\rho_{th}}{\rho_{th}}$	M_{He} ($M_{\odot}$)	$\log(L/L_{\odot})^{tip}$
0.00	0.4753	3.430
0.20	0.4753	3.430
0.25	0.4730	3.424
0.30	0.4612	3.362
0.35	0.4472	3.304
0.40	0.4375	3.255
0.45	0.4308	3.219
0.50	0.4260	3.192

Table 3. Effect of different value for the $^{14}C(\alpha,\gamma)^{18}O$ reaction rate on the evolution of a 0.8 $M_{\odot}$ Z=0.02 model.

$N_A < \sigma v >_{^{14}C,\alpha}$	M_{He} ($M_{\odot}$)	$\log(T_c)$	$\log(\rho_c)$
CF88 $\times 10^{-2}$	0.4604	8.0598	5.8931
CF88 $\times 10^{-1}$	0.4612	8.0599	5.8953
CF88	0.4612	8.0577	5.8964
CF88 $\times 10$	0.4612	8.0577	5.8965
CF88 $\times 10^{2}$	0.4613	8.0584	5.8962

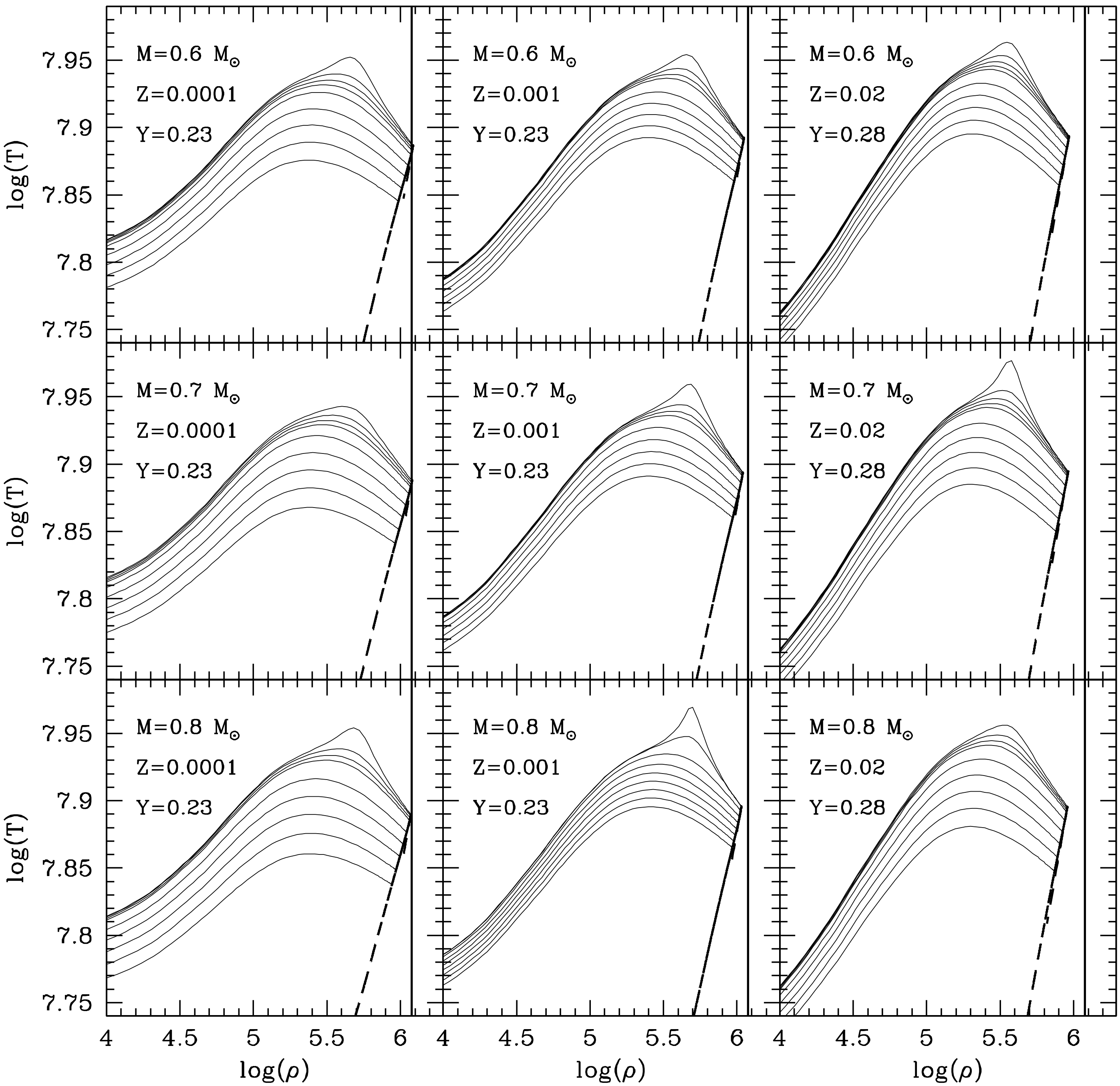
M=0.6 M$_\odot$
Z=0.0001
Y=0.23
M=0.6 M$_\odot$
Z=0.001
Y=0.23
M=0.6 M$_\odot$
Z=0.02
Y=0.28
M=0.7 M$_\odot$
Z=0.0001
Y=0.23
M=0.7 M$_\odot$
Z=0.001
Y=0.23
M=0.7 M$_\odot$
Z=0.02
Y=0.28
M=0.8 M$_\odot$
Z=0.0001
Y=0.23
M=0.8 M$_\odot$
Z=0.001
Y=0.23
M=0.8 M$_\odot$
Z=0.02
Y=0.28
log(T)
log(ρ)

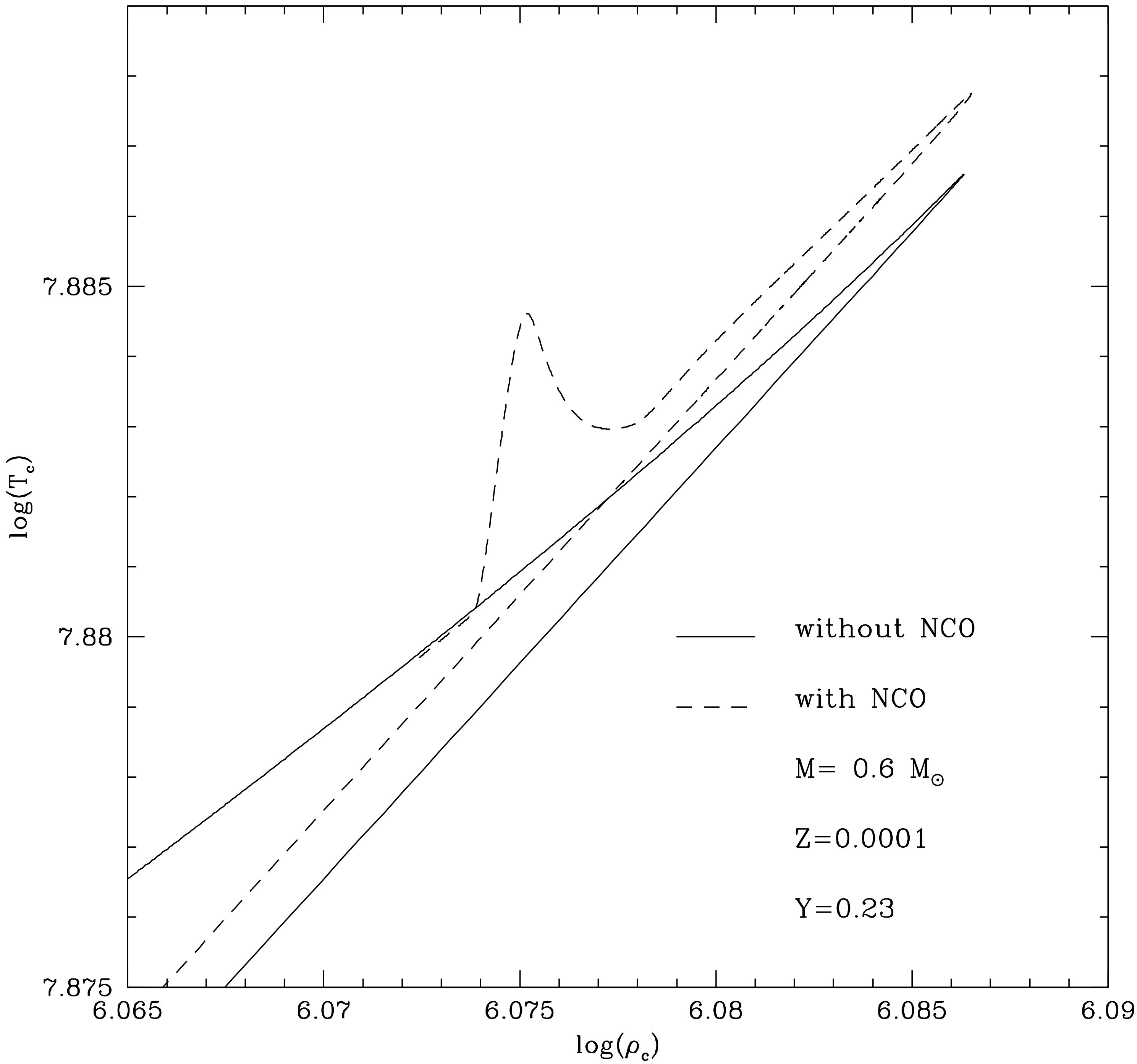

log(T_c)
7.885
7.88
7.875
6.065
6.07
6.075
6.08
6.085
6.09
log(ρ_c)
without NCO
with NCO
M= 0.6 M_⊙
Z=0.0001
Y=0.23

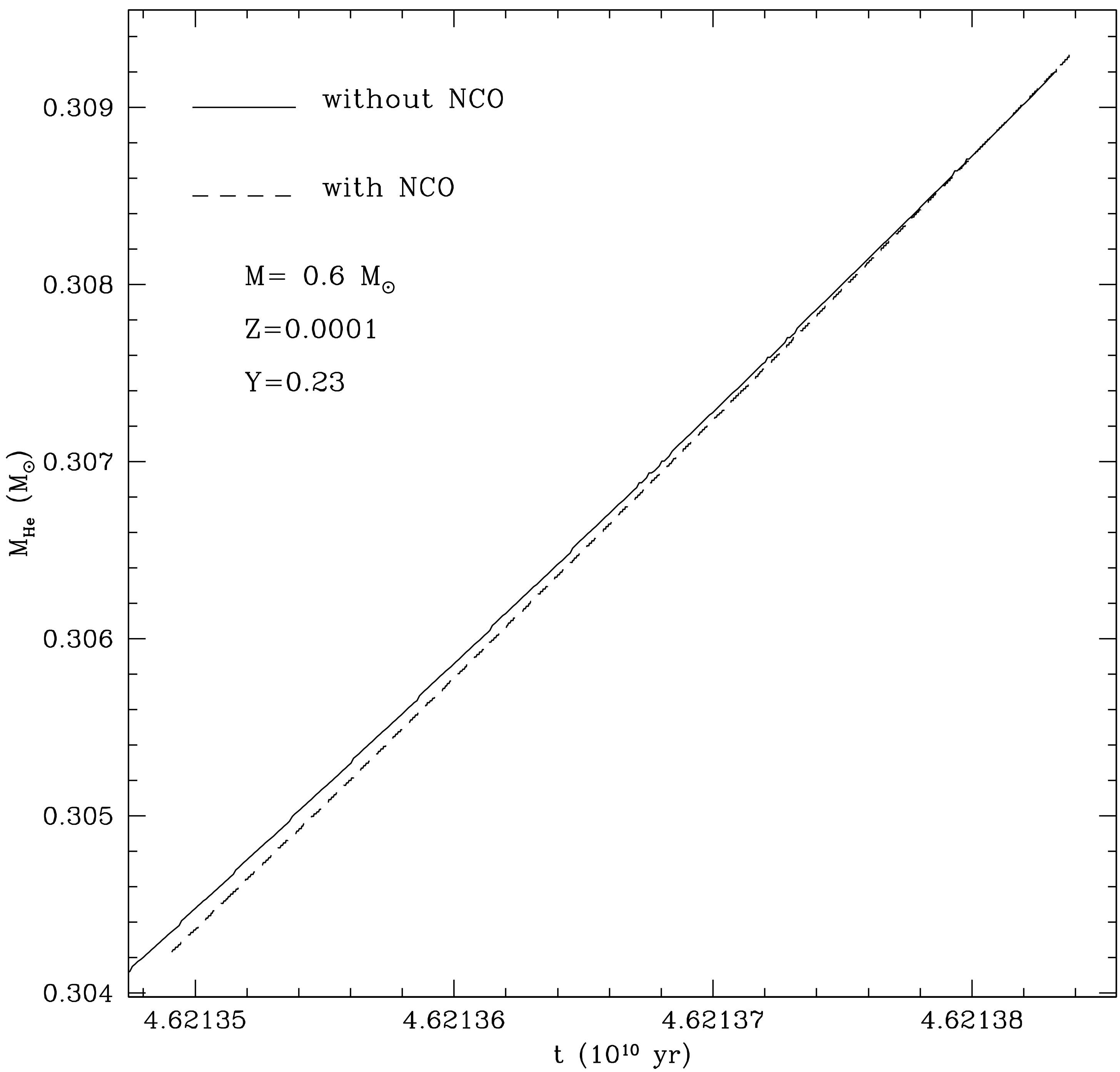

without NCO
with NCO
M= 0.6 $M_\odot$
Z=0.0001
Y=0.23
0.309
0.308
0.307
0.306
0.305
0.304
M_{He} ($M_\odot$)
4.62135
4.62136
4.62137
4.62138
t (10^{10} yr)

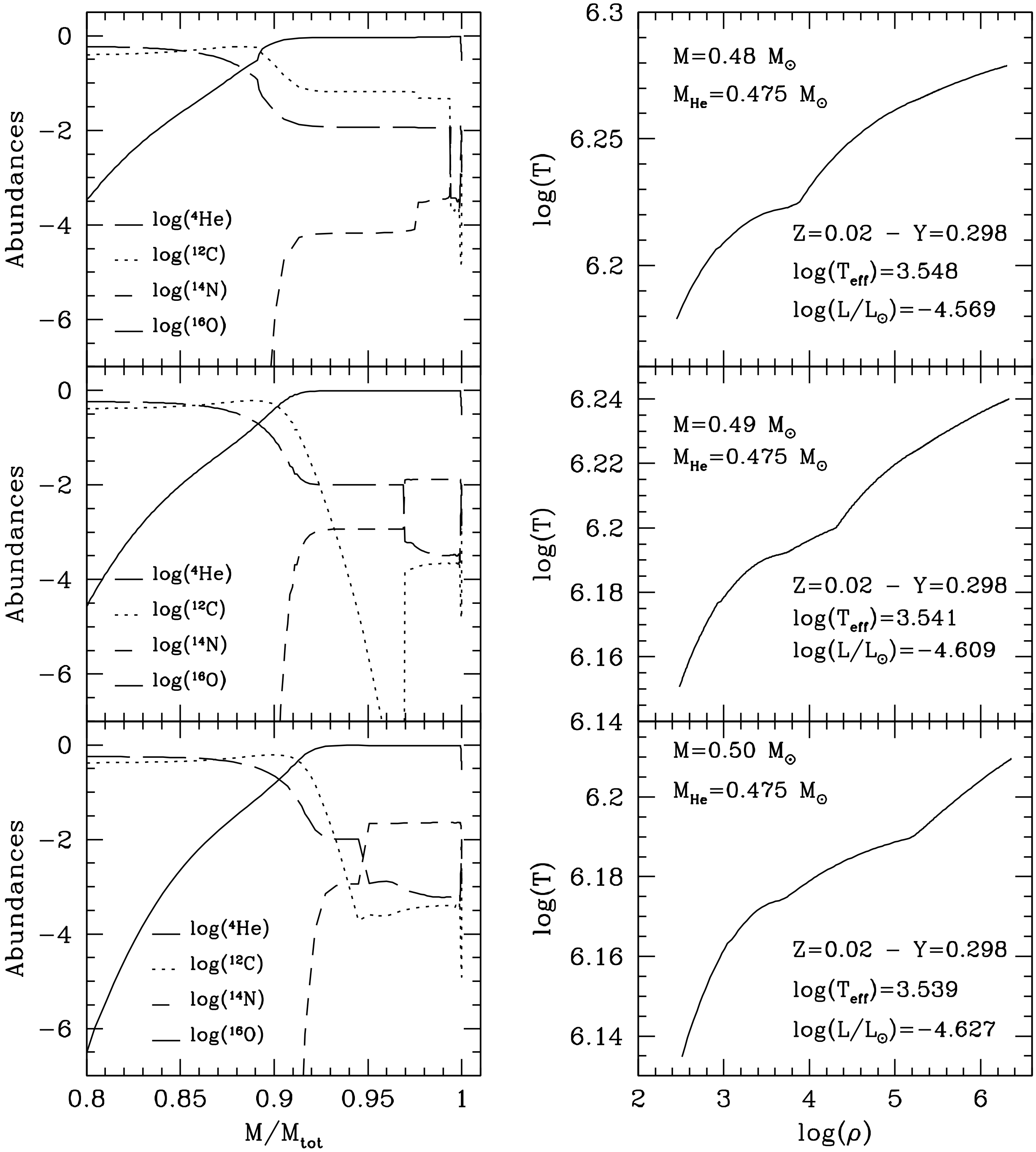

Abundances
log(⁴He)
log(¹²C)
log(¹⁴N)
log(¹⁶O)
M/M_tot
log(T)
log(ρ)
M=0.48 M⊙
M_He=0.475 M⊙
Z=0.02 - Y=0.298
log(T_eff)=3.548
log(L/L⊙)=-4.569
M=0.49 M⊙
M_He=0.475 M⊙
Z=0.02 - Y=0.298
log(T_eff)=3.541
log(L/L⊙)=-4.609
M=0.50 M⊙
M_He=0.475 M⊙
Z=0.02 - Y=0.298
log(T_eff)=3.539
log(L/L⊙)=-4.627

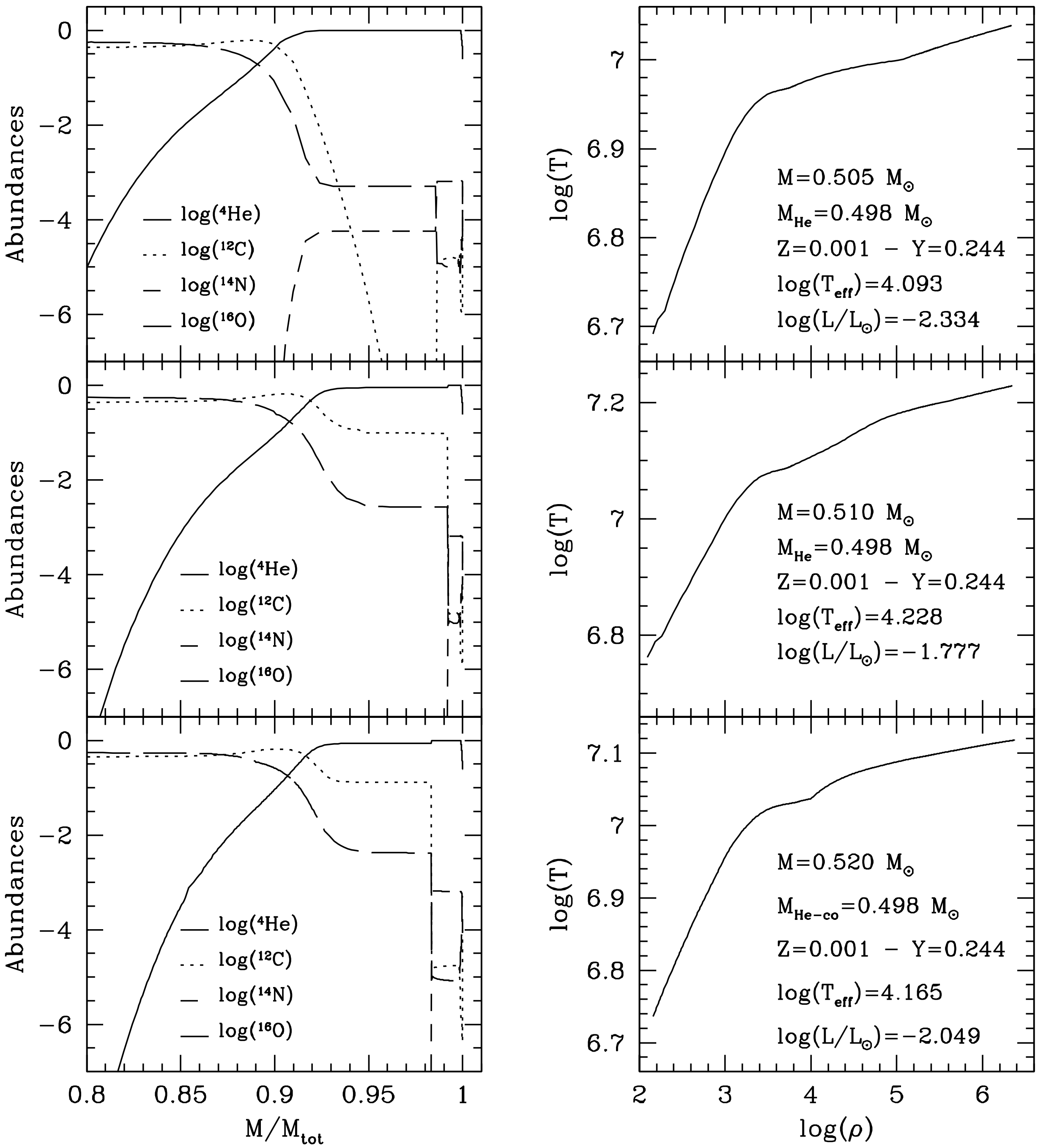

Abundances
log(⁴He)
log(¹²C)
log(¹⁴N)
log(¹⁶O)
M/M_tot
log(T)
log(ρ)
M=0.505 M⊙
M_He=0.498 M⊙
Z=0.001 - Y=0.244
log(T_eff)=4.093
log(L/L⊙)=-2.334
M=0.510 M⊙
M_He=0.498 M⊙
Z=0.001 - Y=0.244
log(T_eff)=4.228
log(L/L⊙)=-1.777
M=0.520 M⊙
M_He-co=0.498 M⊙
Z=0.001 - Y=0.244
log(T_eff)=4.165
log(L/L⊙)=-2.049

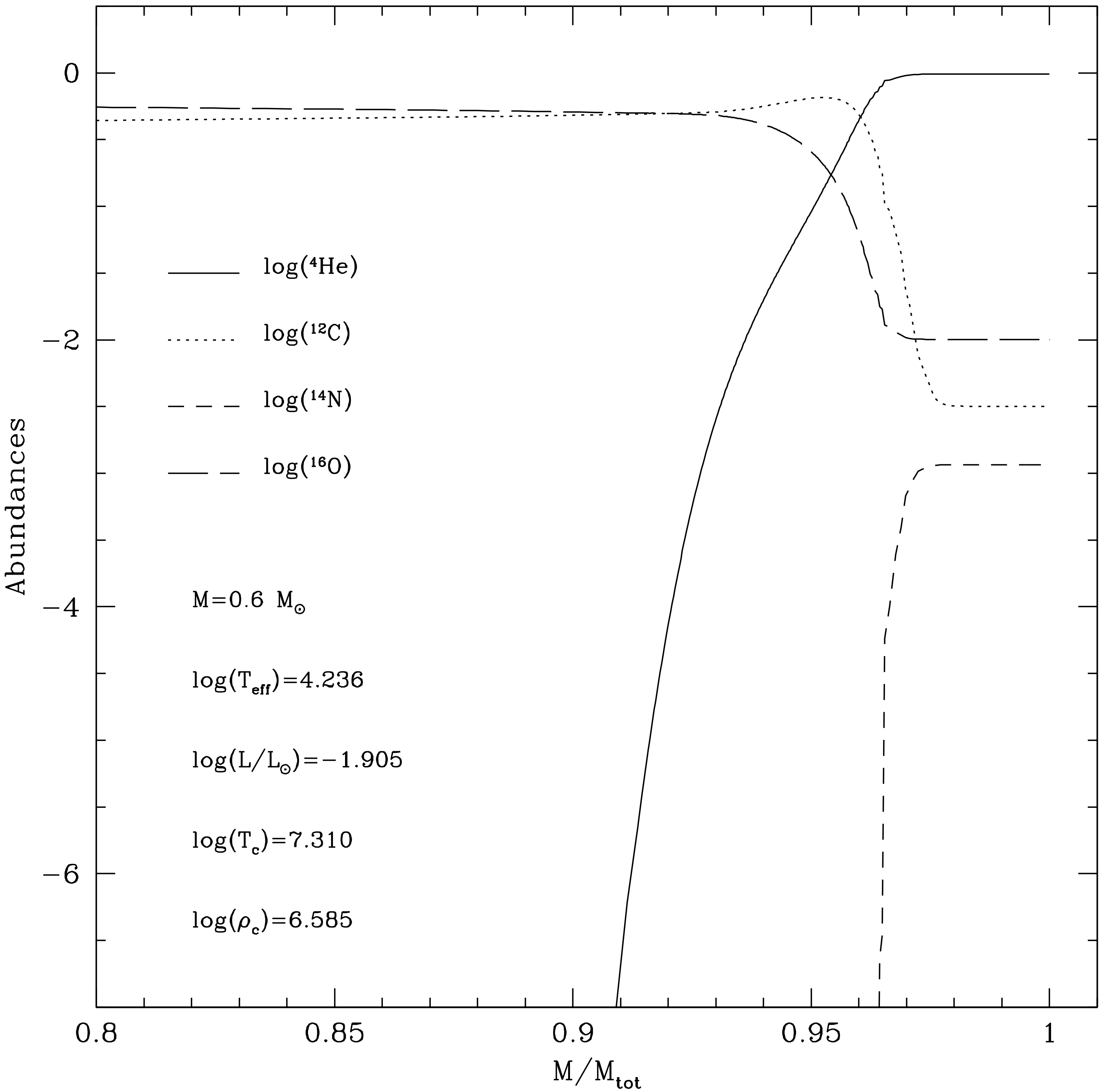

0
−2
−4
−6
0.8
0.85
0.9
0.95
1
M/M$_{tot}$
Abundances
log(^{4}He)
log(^{12}C)
log(^{14}N)
log(^{16}O)
M=0.6 M$_\odot$
log(T$_{eff}$)=4.236
log(L/L$_\odot$)=−1.905
log(T$_c$)=7.310
log(ρ_c)=6.585

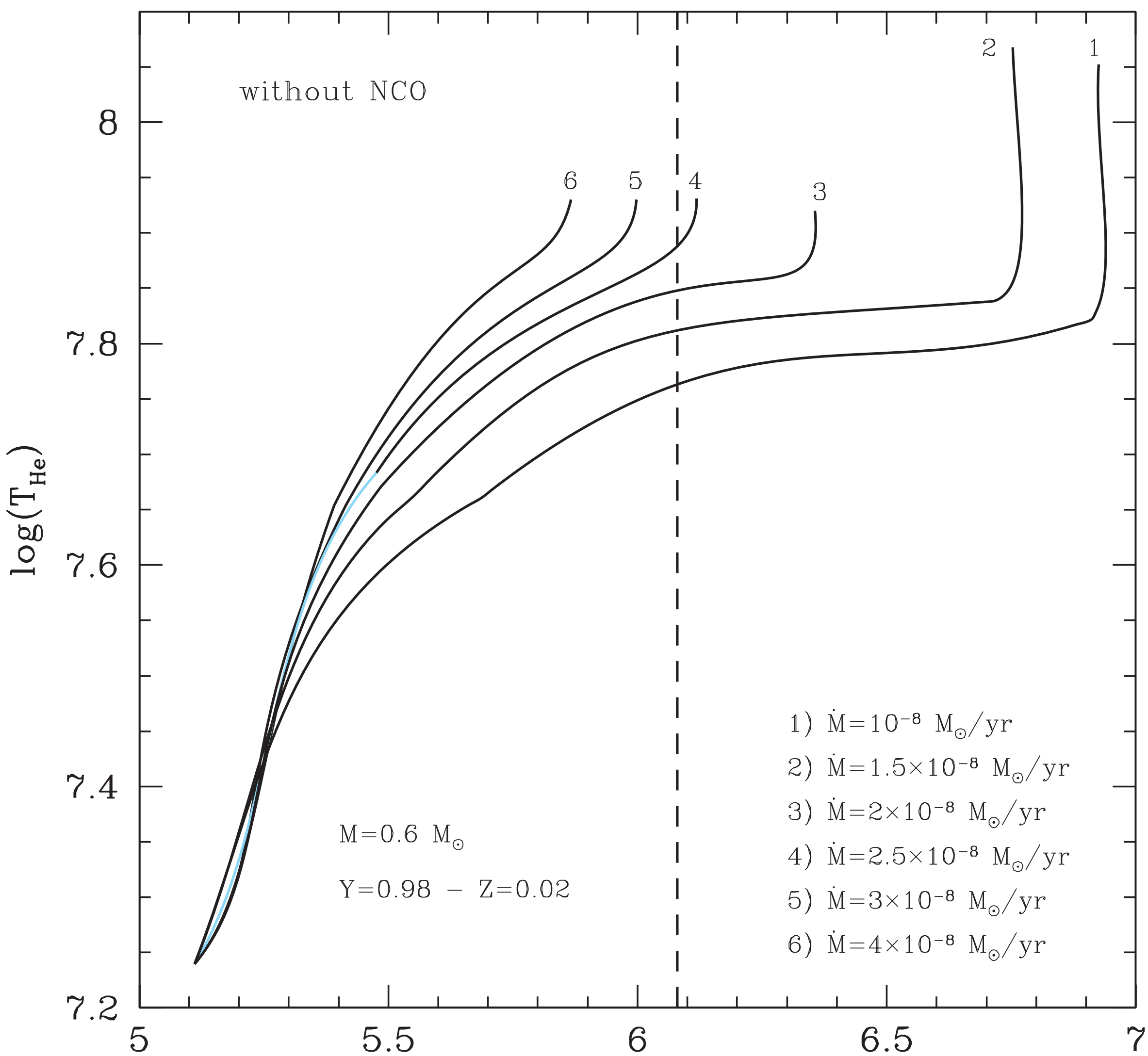

without NCO
1
2
3
4
5
6
M=0.6 M$_\odot$
Y=0.98 – Z=0.02
1) $\dot{M}=10^{-8}$ M$_\odot$/yr
2) $\dot{M}=1.5\times10^{-8}$ M$_\odot$/yr
3) $\dot{M}=2\times10^{-8}$ M$_\odot$/yr
4) $\dot{M}=2.5\times10^{-8}$ M$_\odot$/yr
5) $\dot{M}=3\times10^{-8}$ M$_\odot$/yr
6) $\dot{M}=4\times10^{-8}$ M$_\odot$/yr
log(T$_{He}$)
log(ρ_{He})
7.2
7.4
7.6
7.8
8
5
5.5
6
6.5
7

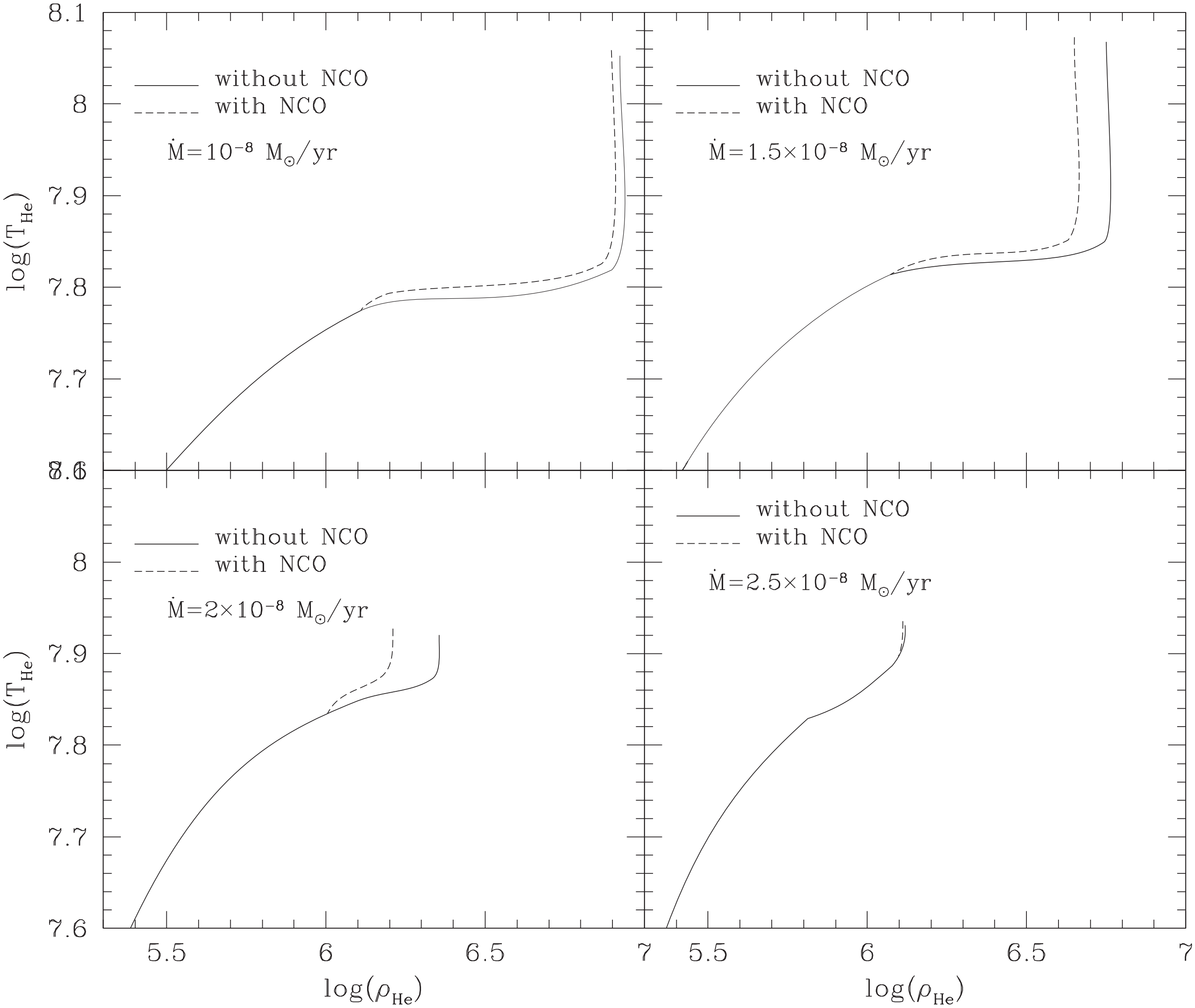

without NCO
with NCO
$\dot{M}=10^{-8}\ M_\odot/yr$
without NCO
with NCO
$\dot{M}=1.5\times10^{-8}\ M_\odot/yr$
without NCO
with NCO
$\dot{M}=2\times10^{-8}\ M_\odot/yr$
without NCO
with NCO
$\dot{M}=2.5\times10^{-8}\ M_\odot/yr$
$\log(T_{He})$
$\log(\rho_{He})$
8.1
8
7.9
7.8
7.7
7.6
5.5
6
6.5
7

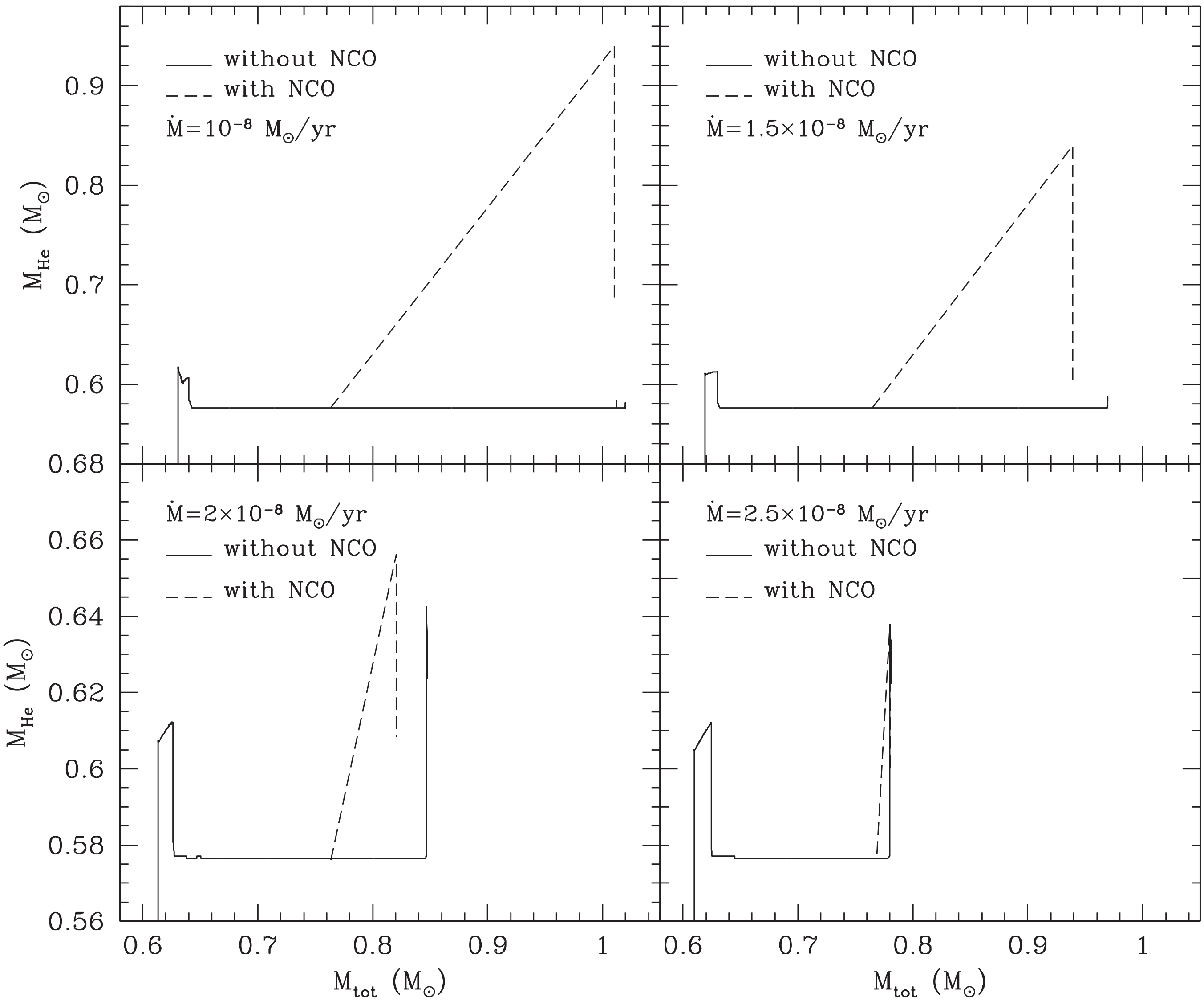

without NCO
with NCO
$\dot{M}=10^{-8}\ M_{\odot}/yr$
without NCO
with NCO
$\dot{M}=1.5\times10^{-8}\ M_{\odot}/yr$
$\dot{M}=2\times10^{-8}\ M_{\odot}/yr$
without NCO
with NCO
$\dot{M}=2.5\times10^{-8}\ M_{\odot}/yr$
without NCO
with NCO
$M_{He}\ (M_{\odot})$
$M_{tot}\ (M_{\odot})$
0.9
0.8
0.7
0.6
0.68
0.66
0.64
0.62
0.6
0.58
0.56
0.6
0.7
0.8
0.9
1

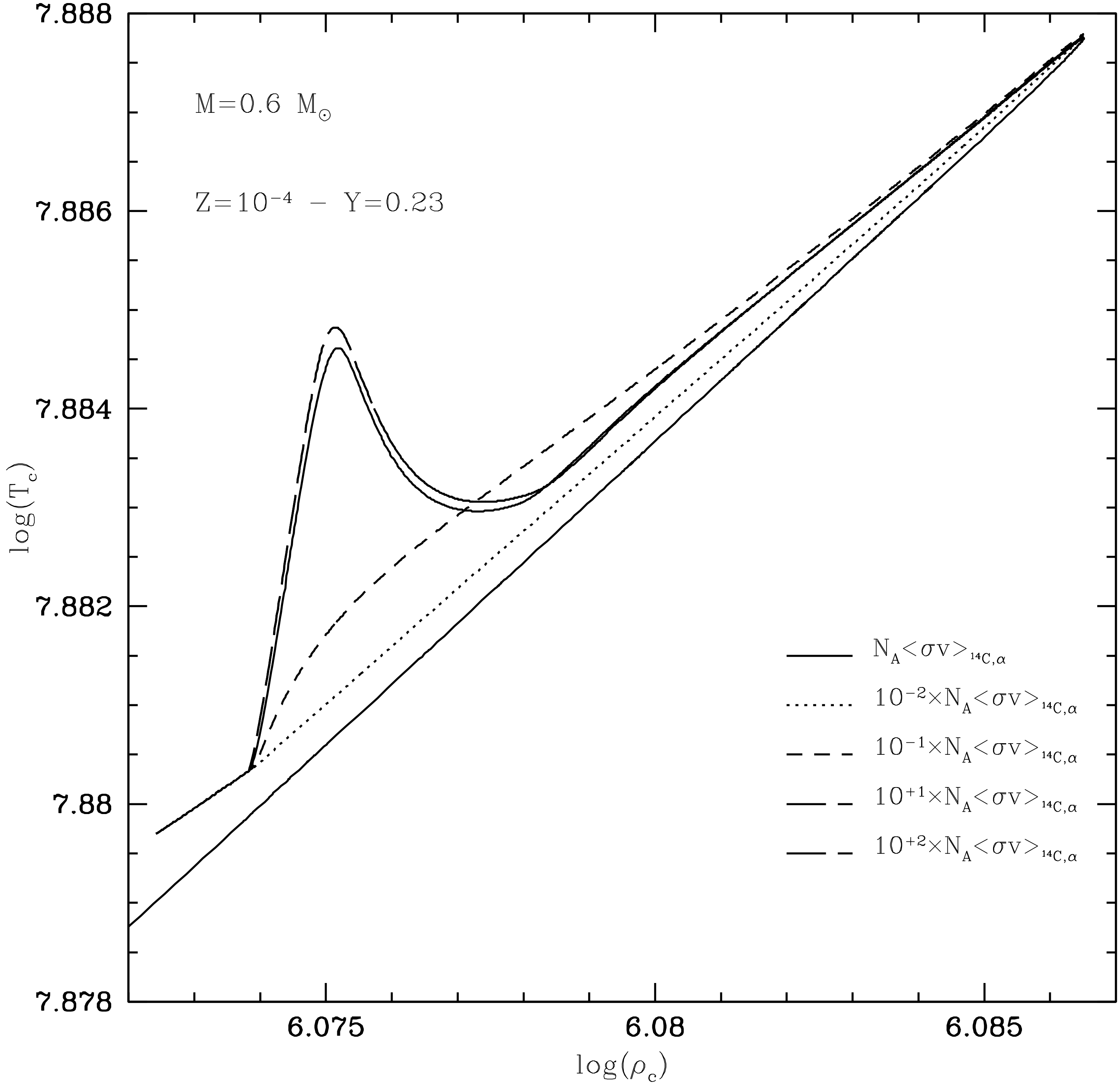

M=0.6 $M_\odot$
Z=10^{-4} – Y=0.23
$N_A<\sigma v>_{^{14}C,\alpha}$
$10^{-2}\times N_A<\sigma v>_{^{14}C,\alpha}$
$10^{-1}\times N_A<\sigma v>_{^{14}C,\alpha}$
$10^{+1}\times N_A<\sigma v>_{^{14}C,\alpha}$
$10^{+2}\times N_A<\sigma v>_{^{14}C,\alpha}$
log(T_c)
log(ρ_c)
7.888
7.886
7.884
7.882
7.88
7.878
6.075
6.08
6.085